

1 **The ionic contribution of proteoglycans to mechanical stiffness of the meniscus**

2 Fahd Mahmood^{1,2}, Jon Clarke², Philip Riches¹

3 1 – Biomedical Engineering Unit, Wolfson Building, University of Strathclyde, 106 Rottenrow,
4 Glasgow, UK, G4 0NW

5 2 – Department of Orthopaedics, Golden Jubilee National Hospital, Agamemnon Street, Clydebank,
6 UK, G81 4DY

7

8 Corresponding author: Fahd Mahmood fahd.mahmood@strath.ac.uk

9

10 **Keywords**

11 Meniscus, proteoglycans, ionic effects, finite element modelling, poroviscoelastic model

12

13 Abstract

14 Load transmission is an important function of the meniscus. In articular cartilage, proteoglycans help
15 maintain hydration via negatively charged moieties. We aimed to investigate the influence of
16 electrostatic effects on stiffness of meniscal tissue.

17 Circular discs from bovine menisci of 8mm diameter and 5mm thickness were placed within a
18 confined compression chamber. The apparatus was bathed in distilled water, 0.14M PBS or 3M PBS
19 before being subjected to 5% ramp compressive strain and held for 300 seconds. FEBio software was
20 used to fit resultant relaxation curves to a non-linear poroviscoelastic model with strain dependent
21 Holmes-Mow permeability. Analysis was conducted using one-way ANOVA with Tukey post-hoc
22 analysis.

23 10 samples were tested in each solution. Significant differences ($p < 0.05$) were observed between
24 the values for Young's modulus, zero strain dependent permeability and the viscoelastic coefficient
25 for samples tested in 3M PBS as compared to deionised water/0.14M PBS. No significant differences
26 were observed in the strain dependent/stiffening coefficients or the relaxation time. Approximately
27 79% of the stiffness of the meniscus appears attributable to ionic effects.

28 Ionic effects play a significant role in the mechanical stiffness of the meniscus. It is important to
29 include the influence of ionic effects when developing mathematical models of this tissue.

30

31 Introduction

32 The menisci of the knee, historically thought of as vestigial remnants [1], are now understood to play
33 a critical role in load transmission across the knee [2–4]. Histologically, the water content of the
34 meniscus is estimated at 74% whilst the remaining dry weight is 75% collagen. Collagen fibres are
35 arranged circumferentially in deeper layers of the tissue and tangentially in superficial layers [5].
36 Load transmitted to the meniscus is resisted by the firm ligamentous attachments of the menisci to
37 bone, generating circumferential tensile (hoop) stresses in the aforementioned circumferential
38 collagen fibres [5,6]. In addition, proteoglycans in the meniscus aid resistance against compressive
39 loading of the meniscus. These large proteins are immobilised in the menisci by the collagen fibres
40 [7] and aid fluid distribution, generating osmotic pressure gradients. Generation of such pressure is
41 also aided by the low permeability of meniscal tissue [5]. Proteoglycans are highly anionic due to
42 their attached glycosaminoglycans, which are present in a variety of connective tissues [8]. The
43 predominant proteoglycan present in the meniscus is chondroitin sulphate, with a smaller
44 proportion of dermatan sulphate also [9]. These types of proteoglycan complexes are similar to
45 those observed in cartilage [10], though the concentrations of proteoglycans within meniscal tissue
46 is lower [11] and has reported to be $1/8^{\text{th}}$ of that in cartilage [12]. Study of porcine menisci suggests
47 that there is a variable concentration of proteoglycans across the width tissue, with the inner surface
48 of the meniscus, which is exposed to the highest loads, demonstrating the highest concentration of
49 proteoglycans [13]. Proteoglycans are thought to be largely responsible for the viscoelastic
50 properties of the meniscus in compression [14].

51 The mechanism through which proteoglycans mediate their effects has been studied in a number of
52 other connective tissues. In articular cartilage and in the nucleus pulposus of the intervertebral disc,
53 proteoglycans exhibit a fixed negative charge due to chondroitin sulphate and keratin sulphate
54 molecules dissociating in solution. In turn, this leads to the development of a high Donnan osmotic
55 pressure in the tissue [15]. This is due to the proteoglycans in the tissue being effectively trapped
56 within the tissue due to their large molecular mass and leads to the tissue itself acting as a semi-
57 permeable membrane. This osmotic pressure leads to an ability of the tissue to resist load. Fluid
58 either exits the tissue (under load) or is re-imbibed (during unloading) to allow the osmotic gradient
59 to reach equilibrium. This swelling is opposed by the collagen fibrillar network, which resists the
60 tension generated by such swelling during loading of the tissue [16].

61 In articular cartilage, depletion of proteoglycans has been shown to result in a reduced compressive
62 modulus [17]. Furthermore, increasing ionic concentration of bathing solutions results in reduced
63 shear modulus of cartilage [18]. Korhonen and Jurvelin [19] tested bovine humeral articular cartilage
64 in solutions of varying ionic concentrations in unconfined compression, fitting a poroelastic biphasic
65 finite element model to demonstrate that an increase in osmolarity of the bathing solution resulted
66 in a decrease in compressive modulus, whilst a decrease resulted in the opposite effect. The authors
67 also showed a correlation between the proteoglycan concentration within the tissue and the
68 compressive modulus measured, hence leading them to suggest that tissue proteoglycans account
69 for a significant proportion of the compressive properties of articular cartilage. Notably, Canal Guterl
70 et al [15] suggest that the Donnan osmotic pressure induced by proteoglycans cannot account for
71 the observed contribution of proteoglycans to tissue stiffness. Through testing of bovine articular
72 cartilage in solutions of varied ionic strengths, coupled with mechanical testing of cartilage before
73 and after proteoglycan digestion, they suggest that the combined electrostatic and non-electrostatic
74 contribution of proteoglycans to the compressive modulus of articular cartilage accounts for >98% of
75 the compressive modulus. Furthermore, ionic effects were thought to represent 62% of this total,
76 with a decrease in the compressive modulus observed in solutions of high ionic concentration.

77 Investigation into the effect of the fixed charge density of proteoglycans within articular cartilage
78 during simulated walking in a finite element model of the knee suggests that the importance of this
79 effect is amplified as the collagen network degenerates, in conditions such as osteoarthritis [20].

80 Proteoglycans are also understood to aid load transmission in the nucleus pulposus of the
81 intervertebral disc, a tissue which withstands significant compressive load in the lumbar spine[21].
82 The structure of proteoglycans within the nucleus pulposus has been found to differ from that
83 observed in other tissues such as articular cartilage or meniscus, with non-aggregated monomers of
84 short length present [22]. However, testing of bovine nucleus pulposus in confined compression in
85 physiological and hypertonic saline solutions suggests that, similar to articular cartilage, the stiffness
86 of nucleus pulposus has both ionic and non-ionic components, with the ionic component responsible
87 for 70% of the stress response [23].

88 The mechanism and extent by which proteoglycans exert this effect has not been demonstrated in
89 meniscal tissue and the contribution of proteoglycans to the mechanical stiffness of the meniscus
90 has not been previously quantified. Such data is important for a complete constitutive description of
91 the tissue enabling appropriate models to be constructed and parameterised. This paper therefore
92 describes a series of experiments to determine the magnitude of the ionic contribution of
93 proteoglycans to mechanical stiffness of the bovine meniscus.

94 Methods

95 Bovine hind legs were obtained from a local abattoir immediately after slaughter. Menisci were
96 excised and immediately frozen at -20°C until the day of testing. Freezing meniscal tissue has been
97 demonstrated to have no significant effect on ultrastructure of the tissue [24] or proteoglycan
98 content [25]. All experiments were conducted within 6 weeks of slaughter. All animal was conducted
99 in accordance with the U.K. Animals (Scientific Procedures) Act, 1986. A circular punch was used to
100 obtain 8 mm diameter cylindrical cores of meniscus in the axial plane from the junction of the
101 middle and outer third of the meniscus. A custom sectioning device was used to cut 5mm thick discs
102 of tissue from these samples. Both femoral and tibial surfaces were removed to generate a mid-
103 substance sample. A micrometre was used to verify sample thickness. Discs were immediately
104 wrapped in a non-permeable plastic film and allowed to defrost for 2 hours.

105 To investigate the influence of ionic effects, we chose to undertake confined compression
106 experiments in solutions of varying ionic concentration. It has been demonstrated that whilst a 3M
107 PBS solution is sufficiently hypertonic to negate ionic effects in both articular cartilage [26] and
108 intervertebral disc [23], whilst a deionised water solution negates all mobile ion effects.

109 Following defrosting, samples were placed into a confined compression chamber, permeable at the
110 bottom only (pore size 400 µm) (Figure 2). Samples were bathed in one of three solutions –
111 deionised water, 0.14M PBS or 3M PBS and immediately subjected to a confined compression
112 protocol as detailed below. The apparatus was placed within a Bose Electroforce 3100 materials
113 testing machine and a custom waveform was created as follows. A porous indenter (pore size 400
114 µm) conforming to the dimensions of the compression chamber was used under load control to
115 apply a preload of 0.3N, followed immediately by a 5% ramp strain under displacement control at
116 1% per second, hence the total strain was applied over 5 seconds for each sample. The strain rate
117 was chosen to allow the requisite strain to be applied without overloading the load cell and was
118 arbitrarily chosen as a balance between the material testing machine's capabilities and requirements
119 of the model used. Both the indenter and compression chamber were comprised of a plastic
120 polymer with a flexural modulus of 3350 N/mm².

121 Separately conducted preliminary testing of samples had established that if subjected solely to a
 122 0.3N preload in 0.14M/3M PBS reached load equilibrium within 1-2 hours, those tested in deionised
 123 water did not reach load equilibrium at >6 hours due to persistent swelling, with swelling effects
 124 becoming dominant at 300 seconds. Hence, to allow samples in each solution to be tested with
 125 similar pre-conditioning, we did not seek to test at load equilibrium, but instead applied a 0.3N
 126 preload followed by an immediate ramp strain compression as detailed above. As swelling effects
 127 became dominant at 300 seconds, relaxation data was collected for only this time period. Hence,
 128 each sample was tested over a ~5 second ramp phase and a 300 second hold phase. Each sample
 129 was tested only once, in one of the three solutions.

130 FEBio software [27] was used to develop a non-linear biphasic poroviscoelastic finite element model
 131 with strain dependent permeability [28]. The model consisted of 404 nodes, with 100 elements. A
 132 convergence study suggested a percentage error of <0.1% for a model with 404 nodes compared to
 133 one with ~1000 nodes, thus a 404 node model was chosen to allow an acceptable compromise
 134 between accuracy and numerical efficiency. Boundary conditions were set to confined compression
 135 and the Poisson's ratio was set to zero. A Poisson's ratio of zero was chosen as it would have no
 136 effect on the experimental results as lateral stresses were not considered. The sides of the chamber,
 137 which were impermeable, were modelled as such, although some lateral flow likely occurred. This
 138 approach is consistent with that used by other authors conducting confined compression
 139 experiments in connective tissues, such as in Ateshian et al's [29] assessment of articular
 140 cartilage, Busby et al's [30] investigation of collagen hydrogels and Heneghan and Riches' [23]
 141 investigation of the intervertebral disc. The material defined has been used to represent the solid
 142 matrix of articular cartilage [29] and intervertebral disc [31]. The coupled hyperelastic strain energy
 143 for this material is given by:

$$W(I_1 I_2 J) = \frac{1}{2} c (e^Q - 1)$$

144 And

$$Q = \frac{\beta}{\lambda + 2\mu} [(2\mu - \lambda)(I_1 - 3) + \lambda(I_2 - 3) - (\lambda + 2\mu) \ln J^2]$$

145 where I_1 and I_2 are the first and second invariants of the right Cauchy-Green tensor, J is the Jacobian
 146 of the deformation gradient and β is the exponential stiffening coefficient. λ and μ are the Lamé
 147 parameters, related to the Young's modulus (E) and Poisson's ratio (ν) as follows:

$$\lambda = \frac{E}{(1 + \nu)(1 - 2\nu)}$$

$$\mu = \frac{E}{2(1 + \nu)}$$

148 The relaxation function (G) was assumed to be given by:

$$G(t) = 1 + \gamma \exp\left(-\frac{t}{\tau}\right)$$

149 where γ is the viscoelastic coefficient and τ is the relaxation time in seconds. Strain dependent
 150 permeability was described by the following function:

$$k(J) = k_0 e^{\frac{1}{2} M (J^2 - 1)}$$

151 where J is the Jacobian of deformation, k_0 is the isotropic hydraulic permeability in the reference
152 state and M is the exponential strain dependent coefficient.

153 The solid stress on the top surface was output and matched to experimental data via a Matlab
154 function, which was written to iteratively reverse engineer appropriate parameters for this model
155 for each relaxation curve using a Nelder-Mead function. Hence the stress relaxation curve for each
156 experiment was used to iteratively determine a best fit line based on mechanical parameters of the
157 poroviscoelastic model, identifying the mechanical parameters which best described the behaviour
158 of the tissue in each given experiment. The exponential strain dependent coefficient and exponential
159 stiffening coefficient were restricted from becoming negative, whilst the power law exponent (α)
160 was held at zero. Resulting best fit parameters were analysed using one way ANOVA with Tukey
161 post-hoc analysis. Significance was set at $p \leq 0.05$. The goodness of fit in the stress relaxation fit was
162 assessed using a coefficient of determination as described by Soltz and Ateshian [32]:

$$R^2 = 1 - \frac{\sum(\sigma - \sigma_{est})^2}{\sum(\sigma - \bar{\sigma})^2}$$

163 where σ is the observed stress, σ_{est} is the estimated variable from the model and $\bar{\sigma}$ is the mean
164 value of σ , summed over all samples time steps.

165 Results

166 Ten samples tested in each solution, with five from derived from the medial meniscus and five from
167 the lateral meniscus, such that a single medial and lateral meniscus was tested in each solution.
168 Mean sample thickness was 5.19 +/- 0.18 mm (s.d.). Mean stress relaxation curves are shown in
169 Figure 1. Table 1 shows mean values for the parameters derived for each sample. There was a
170 significant difference ($p < 0.05$) in the Young's modulus, zero strain dependent permeability and
171 viscoelastic coefficient between samples tested in deionised water/0.14M PBS and those tested in
172 3M PBS. The coefficients of determination in deionised water, 0.14M PBS and 3M PBS were 0.98,
173 0.97 and 0.75 respectively. Based on the relative values of the Young's modulus in 3M PBS compared
174 to 0.14M PBS, approximately 79% of the Young's modulus of bovine meniscus is attributable to ionic
175 effects.

176 Discussion

177 Ionic effects play a significant role in the mechanical stiffness of meniscal tissue. Meniscal tissue is
178 stiffest in 0.14M PBS, the solution which most closely represents the physiological environment. In
179 3M PBS, the elimination of all ionic gradients leads to generation of a larger stress than observed in
180 other solutions. Our results show M or β to be close to zero in all solutions – this likely reflects the
181 small magnitude of strain tested, which suggests the tissue's stiffness is likely constant in the region
182 tested. The viscoelastic coefficient (γ) was also found to be close to zero in 3M PBS rendering the
183 value of τ irrelevant. Notably, our results show that tissue permeability is higher in deionised water,
184 where the effect of mobile ions is negated, than in 0.14M PBS. The reasons for this are unclear and
185 likely reflect an alteration in the complex inter-relationship between the viscoelastic and poroelastic
186 effects within the tissue [33].

187 The coefficient of determination show an excellent fit for data generated in deionised water and
188 0.14M. The 3M data fits the model less well. Biphasic theory assumes tissue to be comprised of two
189 phases – a viscoelastic, porous solid phase and a liquid phase which flows through the solid. If, as our
190 work suggests, electrical charge plays a significant role in modulating the tissue's stiffness, then
191 biphasic theory will not account for such effects. Triphasic [34] or quadriphasic [35] theory may

192 prove a better fit for such tissues, accounting not only for the solid and liquid phases in the tissue,
193 but also for the ionic charge within the tissue. However, the increased number of variables in such
194 models reduces confidence in any variables generated through finite element models, as there is an
195 increased chance of multiple best fit solutions being present.

196 Potential weaknesses of our work include that we obtained samples from all meniscal regions, some
197 authors have suggested that the mechanical properties of meniscal tissue may vary dependent on
198 the region sampled [36]. We attempted to negate any such potential effect by testing a pair of
199 medial/lateral menisci in each solution. We were also unable to test the tissue following a hold
200 phase to allow equilibrium to be achieved due to persistent swelling of the tissue in deionised water
201 at times up to 4 hours – with longer testing times resulting in poorer fit. However, Korhonen and
202 Jurvelin [19] suggest that in fact, the swelling of cartilage tissue in this manner leads to alteration in
203 the pre-tension of collagen fibrils within the solid matrix, which itself may lead to a change in
204 compressive modulus. Our experimental technique negates any such effects. We used fresh frozen
205 tissue and although the literature suggests that freezing meniscus does not alter its structure or
206 proteoglycan content, results obtained using fresh samples may differ from our findings – though
207 such an approach is logistically challenging. The effect of post-mortem time on samples is unknown,
208 though all samples were tested within 6 weeks of slaughter. The post-mortem time was similar
209 between groups such that any confounding effect of post-mortem time would exhibit itself across all
210 groups equally and would hence not affect experimental validity. Finally, we have not assayed our
211 tissues for proteoglycan content and assume that these ionic effects are secondary to the effect of
212 proteoglycans in common with other connective tissues such as cartilage and intervertebral disc.

213 In conclusion, we demonstrate that ionic effects significantly influence the mechanical stiffness of
214 the bovine meniscus, contributing to approximately 79% of the Young's modulus measured in tissue
215 plugs. Although biphasic theory has been used to describe this tissue in the literature, our work
216 suggests that it is necessary to include the influence of ionic effects when developing mathematical
217 models of this tissue, particularly in situations where fluid flow or localised strain is modelled.

218 Competing interests: None declared

219 Funding: None

220 Ethical approval: Not required

221

222 **References**

- 223 [1] Rai MF, McNulty AL. Meniscus beyond mechanics: Using biology to advance our
224 understanding of meniscus injury and treatment. *Connect Tissue Res* 2017;58:221–4.
- 225 [2] Shrive NG, O'Connor JJ, Goodfellow JW. Load-bearing in the knee joint. *Clin Orthop Relat Res*
226 1978;131:279–87.
- 227 [3] Shrive N. The weight bearing role of the menisci of the knee. *J Bone Jt Surgery, Br Vol*
228 1974;56B:381.
- 229 [4] Seedhom BB, Dowson D, Wright V. Functions of the menisci - a preliminary study. *J Bone Jt*
230 *Surgery, Br Vol* 1974;56B:381–2.
- 231 [5] Fithian DC, Kelly MA, Mow VC. Material properties and structure-function relationships in the
232 menisci. *Clin Orthop Relat Res* 1990;252:19–31.

- 233 [6] McDermott ID, Masouros SD, Amis AA. Biomechanics of the menisci of the knee. *Curr Orthop*
234 2008;22:193–201.
- 235 [7] Furumatsu T, Kanazawa T, Yokoyama Y, Abe N, Ozaki T. Inner meniscus cells maintain higher
236 chondrogenic phenotype compared with outer meniscus cells. *Connect Tissue Res*
237 2011;52:459–65.
- 238 [8] Halper J. Proteoglycans and Diseases of Soft Tissues. *Adv. Exp. Med. Biol.*, vol. 802, 2014, p.
239 49–58.
- 240 [9] McDevitt CA, Webber RJ. The ultrastructure and biochemistry of meniscal cartilage. *Clin*
241 *Orthop Relat Res* 1990;252:8–18.
- 242 [10] Roughley PJ, McNicol D, Santer V, Buckwalter J. The presence of a cartilage-like proteoglycan
243 in the adult human meniscus. *Biochem J* 1981;197:77–83.
- 244 [11] Mcnicol D, Roughley PJ. Extraction and Characterization of Proteoglycan from Human
245 Meniscus. *Biochem J* 1980;185:705–13.
- 246 [12] Adams ME, Muir H. The glycosaminoglycans of canine menisci. *Biochem J* 1981;197:385–9.
- 247 [13] Nakano T, Dodd CM, Scott PG. Glycosaminoglycans and proteoglycans from different zones of
248 the porcine knee meniscus. *J Orthop Res* 1997;15:213–20.
- 249 [14] Fox AJS, Wanivenhaus F, Burge AJ, Warren RF, Rodeo SA. The human meniscus: a review of
250 anatomy, function, injury, and advances in treatment. *Clin Anat* 2015;28:269–87.
- 251 [15] Canal Guterl C, Hung CT, Ateshian GA. Electrostatic and non-electrostatic contributions of
252 proteoglycans to the compressive equilibrium modulus of bovine articular cartilage. *J*
253 *Biomech* 2010;43:1343–50.
- 254 [16] Han E, Chen SS, Klisch SM, Sah RL. Contribution of proteoglycan osmotic swelling pressure to
255 the compressive properties of articular cartilage. *Biophys J* 2011;101:916–24.
- 256 [17] Korhonen RK, Laasanen MS, Töyräs J, Lappalainen R, Helminen HJ, Jurvelin JS. Fibril reinforced
257 poroelastic model predicts specifically mechanical behavior of normal, proteoglycan depleted
258 and collagen degraded articular cartilage. *J Biomech* 2003;36:1373–9.
- 259 [18] Parsons JR, Black J. Mechanical behavior of articular cartilage: quantitative changes with
260 alteration of ionic environment. *J Biomech* 1979;12:765–73.
- 261 [19] Korhonen RK, Jurvelin JS. Compressive and tensile properties of articular cartilage in axial
262 loading are modulated differently by osmotic environment. *Med Eng Phys* 2010;32:155–60.
- 263 [20] Räsänen LP, Tanska P, Zbýň Š, van Donkelaar CC, Trattnig S, Nieminen MT, et al. The effect of
264 fixed charge density and cartilage swelling on mechanics of knee joint cartilage during
265 simulated gait. *J Biomech* 2017;61:34–44.
- 266 [21] Wilke HJ, Neef P, Caimi M, Hoogland T, Claes LE. New in vivo measurements of pressures in
267 the intervertebral disc in daily life. *Spine (Phila Pa 1976)* 1999;24:755–62.
- 268 [22] Buckwalter JA, Smith KC, Kazarien LE, Rosenberg LC, Ungar R. Articular cartilage and
269 intervertebral disc proteoglycans differ in structure: An electron microscopic study. *J Orthop*
270 *Res* 1989;7:146–51.
- 271 [23] Heneghan P, Riches PE. The strain-dependent osmotic pressure and stiffness of the bovine
272 nucleus pulposus apportioned into ionic and non-ionic contributors. *J Biomech*
273 2008;41:2411–6.

- 274 [24] Gelber PE, Gonzalez G, Torres R, Garcia Giralto N, Caceres E, Monllau JC. Cryopreservation
275 does not alter the ultrastructure of the meniscus. *Knee Surg Sports Traumatol Arthrosc*
276 2009;17:639–44.
- 277 [25] Qu C, Hirviniemi M, Tiitu V, Jurvelin JS, Töyräs J, Lammi MJ. Effects of Freeze-Thaw Cycle with
278 and without Proteolysis Inhibitors and Cryopreservant on the Biochemical and Biomechanical
279 Properties of Articular Cartilage. *Cartilage* 2014;5:97–106.
- 280 [26] Mow VC, Schoonbeck JM. Contribution of Donnan osmotic pressure towards the biphasic
281 compressive modulus of articular cartilage. *Trans Orthop Res Soc* 1984;9:262.
- 282 [27] Maas SA, Ellis BJ, Ateshian GA, Weiss JA. FEBio: Finite Elements for Biomechanics. *J Biomech*
283 *Eng* 2012;134:011005.
- 284 [28] Holmes MH, Mow VC. The nonlinear characteristics of soft gels and hydrated connective
285 tissues in ultrafiltration. *J Biomech* 1990;23:1145–56.
- 286 [29] Ateshian GA, Warden WH, Kim JJ, Grelsamer RP, Mow VC. Finite deformation biphasic
287 material properties of bovine articular cartilage from confined compression experiments. *J*
288 *Biomech* 1997;30:1157–64.
- 289 [30] Busby GA, Grant MH, MacKay SP, Riches PE. Confined compression of collagen hydrogels. *J*
290 *Biomech* 2013;46:837–40.
- 291 [31] Iatridis JC, Setton LA, Foster RJ, Rawlins BA, Weidenbaum M, Mow VC. Degeneration affects
292 the anisotropic and nonlinear behaviors of human annulus fibrosus in compression. *J Biomech*
293 1998;31:535–44.
- 294 [32] Soltz MA, Ateshian GA. Interstitial Fluid Pressurization During Confined Compression Cyclical
295 Loading of Articular Cartilage. *J Biomech* 1998;31:927–34.
- 296 [33] Hosseini SM, Wilson W, Ito K, van Donkelaar CC. How preconditioning affects the
297 measurement of poro-viscoelastic mechanical properties in biological tissues. *Biomech Model*
298 *Mechanobiol* 2013;13:503–13.
- 299 [34] Lai WM, Hou JS, Mow VC. A triphasic theory for the swelling and deformation behaviors of
300 articular cartilage. *J Biomech Eng* 1991;113:245–58.
- 301 [35] Huyghe JM, Janssen J. Quadriphasic mechanics of swelling incompressible porous media. *Int J*
302 *Eng Sci* 1997;35:793–802.
- 303 [36] Proctor CS, Schmidt MB, Whipple RR, Kelly MA, Mow VC. Material properties of the normal
304 medial bovine meniscus. *J Orthop Res* 1989;7:771–82.
- 305
- 306

1 **The ionic contribution of proteoglycans to mechanical stiffness of the meniscus**

2 Fahd Mahmood^{1,2}, Jon Clarke², Philip Riches¹

3 1 – Biomedical Engineering Unit, Wolfson Building, University of Strathclyde, 106 Rottenrow,
4 Glasgow, UK, G4 0NW

5 2 – Department of Orthopaedics, Golden Jubilee National Hospital, Agamemnon Street, Clydebank,
6 UK, G81 4DY

7

8 Corresponding author: Fahd Mahmood fahd.mahmood@strath.ac.uk

9

10 **Keywords**

11 Meniscus, proteoglycans, ionic effects, finite element modelling, poroviscoelastic model

12

13 Abstract

14 Load transmission is an important function of the meniscus. In articular cartilage, proteoglycans help
15 maintain hydration via negatively charged moieties. We aimed to investigate the ~~role of~~
16 ~~proteoglycans in~~influence of electrostatic effects on stiffness of meniscal tissue.

17 ~~8mm diameter, 5mm thick circular~~Circular discs from bovine menisci of 8mm diameter and 5mm
18 thickness were placed within a confined compression chamber. The apparatus was bathed in
19 distilled water, 0.14M PBS or 3M PBS before being subjected to 5% ramp compressive strain and
20 held for 300 seconds. FEBio software was used to fit resultant relaxation curves to a non-linear
21 poroviscoelastic model with strain dependent Holmes-Mow permeability. Analysis was conducted
22 using one-way ANOVA with Tukey post-hoc analysis.

23 10 samples were tested in each solution. Significant differences ($p < 0.05$) were observed between
24 the values for Young's modulus, zero strain dependent permeability and the viscoelastic coefficient
25 for samples tested in 3M PBS as compared to deionised water/0.14M PBS. No significant differences
26 were observed in the strain dependent/stiffening coefficients or the relaxation time. Approximately
27 79% of the stiffness of the meniscus appears attributable to ionic effects.

28 Ionic effects play a significant role in the mechanical stiffness of the meniscus. It is important to
29 include the influence of ionic effects when developing mathematical models of this tissue.

30

31 Introduction

32 The menisci of the knee, historically thought of as vestigial remnants [1], are now understood to play
33 a critical role in load transmission across the knee [2–4]. Histologically, the water content of the
34 meniscus is estimated at 74% whilst the remaining dry weight is 75% collagen. Collagen fibres are
35 arranged circumferentially in deeper layers of the tissue and tangentially in superficial layers [5].
36 Load transmitted to the meniscus is resisted by the firm ligamentous attachments of the menisci to
37 bone, generating circumferential tensile (hoop) stresses in the aforementioned circumferential
38 collagen fibres [5,6]. In addition, proteoglycans in the meniscus aid resistance against compressive
39 loading of the meniscus. These large proteins are immobilised in the menisci by the collagen fibres
40 [7] and aid fluid distribution, generating osmotic pressure gradients. Generation of such pressure is
41 also aided by the low permeability of meniscal tissue [5]. Proteoglycans are highly anionic due to
42 their attached glycosaminoglycans, which are present in a variety of connective tissues [8]. The
43 predominant proteoglycan present in the meniscus is chondroitin sulphate, with a smaller
44 proportion of dermatan sulphate also [9]. These types of proteoglycan complexes are similar to
45 those observed in cartilage [10], though the concentrations of proteoglycans within meniscal tissue
46 is lower [11] and has reported to be $1/8^{\text{th}}$ of that in cartilage [12]. Study of porcine menisci suggests
47 that there is a variable concentration of proteoglycans across the width tissue, with the inner surface
48 of the meniscus, which is exposed to the highest loads, demonstrating the highest concentration of
49 proteoglycans [13]. Proteoglycans are thought to be largely responsible for the viscoelastic
50 properties of the meniscus in compression [14].

51 The mechanism through which proteoglycans mediate their effects has been studied in a number of
52 other connective tissues. In articular cartilage and in the nucleus pulposus of the intervertebral disc,
53 proteoglycans exhibit a fixed negative charge due to chondroitin sulphate and keratin sulphate
54 molecules dissociating in solution. In turn, this leads to the development of a high Donnan osmotic
55 pressure in the tissue [15]. This is due to the proteoglycans in the tissue being effectively trapped
56 within the tissue due to their large molecular mass and leads to the tissue itself acting as a semi-
57 permeable membrane. This osmotic pressure leads to an ability of the tissue to resist load. Fluid
58 either exits the tissue (under load) or is re-imbibed (during unloading) to allow the osmotic gradient
59 to reach equilibrium. This swelling is opposed by the collagen fibrillar network, which resists the
60 tension generated by such swelling during loading of the tissue [16].

61 In articular cartilage, depletion of proteoglycans has been shown to result in a reduced compressive
62 modulus [17]. Furthermore, increasing ionic concentration of bathing solutions results in reduced
63 shear modulus of cartilage [18]. Korhonen and Jurvelin [19] tested bovine humeral articular cartilage
64 in solutions of varying ionic concentrations in unconfined compression, fitting a poroelastic biphasic
65 finite element model to demonstrate that an increase in osmolarity of the bathing solution resulted
66 in a decrease in compressive modulus, whilst a decrease resulted in the opposite effect. The authors
67 also showed a correlation between the proteoglycan concentration within the tissue and the
68 compressive modulus measured, hence leading them to suggest that tissue proteoglycans account
69 for a significant proportion of the compressive properties of articular cartilage. Notably, Canal Guterl
70 et al [15] suggest that the Donnan osmotic pressure induced by proteoglycans cannot account for
71 the observed contribution of proteoglycans to tissue stiffness. Through testing of bovine articular
72 cartilage in solutions of varied ionic strengths, coupled with mechanical testing of cartilage before
73 and after proteoglycan digestion, they suggest that the combined electrostatic and non-electrostatic
74 contribution of proteoglycans to the compressive modulus of articular cartilage accounts for >98% of
75 the compressive modulus. Furthermore, ionic effects were thought to represent 62% of this total,
76 with a decrease in the compressive modulus observed in solutions of high ionic concentration.

77 Investigation into the effect of the fixed charge density of proteoglycans within articular cartilage
78 during simulated walking in a finite element model of the knee suggests that the importance of this
79 effect is amplified as the collagen network degenerates, in conditions such as osteoarthritis [20].

80 Proteoglycans are also understood to aid load transmission in the nucleus pulposus of the
81 intervertebral disc, a tissue which withstands significant compressive load in the lumbar spine [21].
82 The structure of proteoglycans within the nucleus pulposus has been found to differ from that
83 observed in other tissues such as articular cartilage or meniscus, with non-aggregated monomers of
84 short length present [22]. However, testing of bovine nucleus pulposus in confined compression in
85 physiological and hypertonic saline solutions suggests that, similar to articular cartilage, the stiffness
86 of nucleus pulposus has both ionic and non-ionic components, with the ionic component responsible
87 for 70% of the stress response [23].

88 The mechanism and extent by which proteoglycans exert this effect has not been demonstrated in
89 meniscal tissue and the contribution of proteoglycans to the mechanical stiffness of the meniscus
90 has not been previously quantified. Such data is important for a complete constitutive description of
91 the tissue enabling appropriate models to be constructed and parameterised. This paper therefore
92 describes a series of experiments to determine the magnitude of the ionic contribution of
93 proteoglycans to mechanical stiffness of the bovine meniscus.

94 Methods

95 Bovine hind legs were obtained from a local abattoir immediately after slaughter. Menisci were
96 excised and immediately frozen at -20°C until the day of testing. Freezing meniscal tissue has been
97 demonstrated to have no significant effect on ultrastructure of the tissue [24] or proteoglycan
98 content [25]. All experiments were conducted within 6 weeks of slaughter. All animal was conducted
99 in accordance with the U.K. Animals (Scientific Procedures) Act, 1986. A circular punch was used to
100 obtain 8 mm diameter cylindrical cores of meniscus in the axial plane from the junction of the
101 middle and outer third of the meniscus. A custom sectioning device was used to cut 5mm thick discs
102 of tissue from these samples. Both femoral and tibial surfaces were removed to generate a mid-
103 substance sample. A micrometre was used to verify sample thickness. Discs were immediately
104 wrapped in a non-permeable plastic film and allowed to defrost for 2 hours.

105 To investigate the influence of ionic effects, we chose to undertake confined compression
106 experiments in solutions of varying ionic concentration. It has been demonstrated that whilst a 3M
107 PBS solution is sufficiently hypertonic to negate ionic effects in both articular cartilage [26] and
108 intervertebral disc [23], whilst a deionised water solution negates all mobile ion effects.

109 Following defrosting, samples were placed into a confined compression chamber ~~with~~, permeable at
110 the bottom only (pore size 400 µm) ~~and~~ (Figure 2). Samples were bathed in one of three solutions –
111 deionised water, 0.14M PBS or 3M PBS ~~and immediately subjected to a confined compression~~
112 protocol as detailed below. The apparatus was placed within a Bose Electroforce 3100 materials
113 testing machine and a custom waveform was created as follows. A porous indenter (pore size 400
114 µm) ~~was used~~ conforming to the dimensions of the compression chamber was used under load
115 control to apply a preload of 0.3N, followed immediately by a 5% ramp strain under displacement
116 control at 1% per second ~~–Preliminary, hence the total strain was applied over 5 seconds for each~~
117 sample. The strain rate was chosen to allow the requisite strain to be applied without overloading
118 the load cell and was arbitrarily chosen as a balance between the material testing machine's
119 capabilities and requirements of the model used. Both the indenter and compression chamber were
120 comprised of a plastic polymer with a flexural modulus of 3350 N/mm².

121 Separately conducted preliminary testing of samples had established that ~~whilst samples if subjected~~
 122 solely to a 0.3N preload in 0.14M/3M PBS reached load equilibrium within 1-2 hours, those tested in
 123 deionised water did not reach load equilibrium at >6 hours. ~~These tests also demonstrated that due~~
 124 to persistent swelling, with swelling effects becoming dominant at 300 seconds. Hence, to allow
 125 samples in each solution to be tested with similar pre-conditioning, we did not seek to test at load
 126 equilibrium, but instead applied a 0.3N preload followed by an immediate ramp strain compression
 127 as detailed above. As swelling effects became dominant at 300 seconds. Hence, samples were
 128 allowed to relax for 300 seconds., relaxation data was collected for only this time period. Hence,
 129 each sample was tested over a ~5 second ramp phase and a 300 second hold phase. Each sample
 130 was tested only once, in one of the three solutions.

131 FEBio software [27] was used to develop a non-linear biphasic poroviscoelastic finite element model
 132 with strain dependent permeability [28]. The model consisted of 404 nodes, with 100 elements. A
 133 convergence study suggested a percentage error of <0.1% for a model with 404 nodes compared to
 134 one with ~1000 nodes, thus a 404 node model was chosen to allow an acceptable compromise
 135 between accuracy and numerical efficiency. Boundary conditions were set to confined compression
 136 and the Poisson's ratio was set to zero. A Poisson's ratio of zero was chosen as it would have no
 137 effect on the experimental results as lateral stresses were not considered. The sides of the chamber,
 138 which were impermeable, were modelled as such, although some lateral flow likely occurred. This
 139 approach is consistent with that used by other authors conducting confined compression
 140 experiments in connective tissues, such as in Ateshian et al's [29] assessment of articular cartilage,
 141 Busby et al's [30] investigation of collagen hydrogels and Heneghan and Riches' [23] investigation of
 142 the intervertebral disc. The material defined has been used to represent the solid matrix of articular
 143 cartilage [29] and intervertebral disc [31]. The coupled hyperelastic strain energy for this material is
 144 given by:

$$W(I_1, I_2, J) = \frac{1}{2} c (e^Q - 1)$$

145 And

$$Q = \frac{\beta}{\lambda + 2\mu} [(2\mu - \lambda)(I_1 - 3) + \lambda(I_2 - 3) - (\lambda + 2\mu) \ln J^2]$$

146 where I_1 and I_2 are the first and second invariants of the right Cauchy-Green tensor, J is the Jacobian
 147 of the deformation gradient and β is the exponential stiffening coefficient. λ and μ are the Lamé
 148 parameters, related to the Young's modulus (E) and Poisson's ratio (ν) as follows:

$$\lambda = \frac{E}{(1 + \nu)(1 - 2\nu)}$$

$$\mu = \frac{E}{2(1 + \nu)}$$

149 The relaxation function (G) was assumed to be given by:

$$G(t) = 1 + \gamma \exp\left(-\frac{t}{\tau}\right)$$

150 where γ is the viscoelastic coefficient and τ is the relaxation time in seconds. Strain dependent
 151 permeability was described by the following function:

$$k(J) = k_0 e^{\frac{1}{2} M (J^2 - 1)}$$

152 where J is the Jacobian of deformation, k_0 is the isotropic hydraulic permeability in the reference
153 state and M is the exponential strain dependent coefficient.

154 The solid stress on the top surface was ~~outputted~~ ~~output~~ and matched to experimental data via a
155 Matlab function, which was written to iteratively reverse engineer appropriate parameters for this
156 model for each relaxation curve using a Nelder-Mead function. Hence the stress relaxation curve for
157 each experiment was used to iteratively determine a best fit line based on mechanical parameters of
158 the poroviscoelastic model, identifying the mechanical parameters which best described the
159 behaviour of the tissue in each given experiment. The exponential strain dependent coefficient and
160 exponential stiffening coefficient were restricted from becoming negative, whilst the power law
161 exponent (α) was held at zero. Resulting best fit parameters were analysed using one way ANOVA
162 with Tukey post-hoc analysis. Significance was set at $p \leq 0.05$. The goodness of fit in the stress
163 relaxation fit was assessed using a coefficient of determination as described by Soltz and Ateshian
164 [28][32]:

$$R^2 = 1 - \frac{\sum(\sigma - \sigma_{est})^2}{\sum(\sigma - \bar{\sigma})^2}$$

165 where σ is the observed stress, σ_{est} is the estimated variable from the model and $\bar{\sigma}$ is the mean
166 value of σ , summed over all samples time steps.

167 Results

168 ~~40~~ Ten samples tested in each solution, with ~~5~~ five from derived from the medial meniscus and ~~5~~ five
169 from the lateral meniscus, such that a single medial and lateral meniscus was tested in each solution.
170 Mean sample thickness was 5.19 +/- 0.18 mm ~~-(s.d.)~~. Mean stress relaxation curves are shown in
171 Figure 1. Table 1 shows mean values for the parameters derived for each sample. There was a
172 significant difference ($p < 0.05$) in the Young's modulus, zero strain dependent permeability and
173 viscoelastic coefficient between samples tested in deionised water/0.14M PBS and those tested in
174 3M PBS. The coefficients of determination in deionised water, 0.14M PBS and 3M PBS were 0.98,
175 0.97 and 0.75 respectively. Approximately Based on the relative values of the Young's modulus in 3M
176 PBS compared to 0.14M PBS, approximately 79% of the Young's modulus of bovine meniscus is
177 attributable to ionic effects.

178 Discussion

179 Ionic effects play a significant role in the mechanical stiffness of meniscal tissue. Meniscal tissue is
180 stiffest in 0.14M PBS, the solution which most closely represents the physiological environment. In
181 3M PBS, the elimination of all ionic gradients leads to generation of a larger stress than observed in
182 other solutions. Our results show M or β to be close to zero in all solutions – this likely reflects the
183 small magnitude of strain tested, which suggests the tissue's stiffness is likely constant in the region
184 tested. The viscoelastic coefficient (γ) was also found to be close to zero in 3M PBS rendering the
185 value of τ irrelevant. Notably, our results show that tissue permeability is higher in deionised water,
186 where the effect of mobile ions is negated, than in 0.14M PBS. The reasons for this are unclear and
187 likely reflect an alteration in the complex inter-relationship between the viscoelastic and poroelastic
188 effects within the tissue [29]-[33].

189 The coefficient of determination show an excellent fit for data generated in deionised water and
190 0.14M. The 3M data fits the model less well. Biphasic theory assumes tissue to be comprised of two
191 phases – a viscoelastic, porous solid phase and a liquid phase which flows through the solid. If, as our
192 work suggests, electrical charge plays a significant role in in modulating the tissue's stiffness, then

Field Code Changed

193 | biphasic theory will not account for such effects. Triphasic [30][34] or quadriphasic [34][35] theory
194 | may prove a better fit for such tissues, accounting not only for the solid and liquid phases in the
195 | tissue, but also for the ionic charge within the tissue. However, the increased number of variables in
196 | such models reduces confidence in any variables generated through finite element models, as there
197 | is an increased chance of multiple best fit solutions being present.

198 | Potential weaknesses of our work include that we obtained samples from all meniscal regions, some
199 | authors have suggested that the mechanical properties of meniscal tissue may vary dependent on
200 | the region sampled [32]-[36]. We attempted to negate any such potential effect by testing a pair of
201 | medial/lateral menisci in each solution. We were also unable to test the tissue following a hold
202 | phase to allow equilibrium to be achieved due to persistent swelling of the tissue in deionised water
203 | at times up to 4 hours – with longer testing times resulting in poorer fit. However, Korhonen and
204 | Jurvelin [19][19] suggest that in fact, the swelling of cartilage tissue in this manner leads to alteration
205 | in the pre-tension of collagen fibrils within the solid matrix, which itself may lead to a change in
206 | compressive modulus. ~~Our experimental technique negates any such effects. Our experimental~~
207 | ~~technique negates any such effects. We used fresh frozen tissue and although the literature suggests~~
208 | ~~that freezing meniscus does not alter its structure or proteoglycan content, results obtained using~~
209 | ~~fresh samples may differ from our findings – though such an approach is logistically challenging. The~~
210 | ~~effect of post-mortem time on samples is unknown, though all samples were tested within 6 weeks~~
211 | ~~of slaughter. The post-mortem time was similar between groups such that any confounding effect of~~
212 | ~~post-mortem time would exhibit itself across all groups equally and would hence not affect~~
213 | ~~experimental validity.~~ Finally, we have not assayed our tissues for proteoglycan content and assume
214 | that these ionic effects are secondary to the effect of proteoglycans in common with other
215 | connective tissues such as cartilage and intervertebral disc.

216 | In conclusion, we demonstrate that ionic effects significantly influence the mechanical stiffness of
217 | the bovine meniscus, contributing to approximately 79% of the Young's modulus measured in tissue
218 | plugs. Although biphasic theory has been used to describe this tissue in the literature, our work
219 | suggests that it is necessary to include the influence of ionic effects when developing mathematical
220 | models of this tissue, particularly in situations where fluid flow or localised strain is modelled.

221 | Competing interests: None declared

222 | Funding: None

223 | Ethical approval: Not required

224 | **References**

- 225 | [1] Rai MF, McNulty AL. Meniscus beyond mechanics: Using biology to advance our
226 | understanding of meniscus injury and treatment. *Connect Tissue Res* 2017;58:221–4.
- 227 | [2] Shrive NG, O'Connor JJ, Goodfellow JW. Load-bearing in the knee joint. *Clin Orthop Relat Res*
228 | 1978;131:279–87.
- 229 | [3] Shrive N. The weight bearing role of the menisci of the knee. *J Bone Jt Surgery, Br Vol*
230 | 1974;56B:381.
- 231 | [4] Seedhom BB, Dowson D, Wright V. Functions of the menisci - a preliminary study. *J Bone Jt*
232 | *Surgery, Br Vol* 1974;56B:381–2.
- 233 | [5] Fithian DC, Kelly MA, Mow VC. Material properties and structure-function relationships in the
234 | menisci. *Clin Orthop Relat Res* 1990;252:19–31.

- 235 [6] McDermott ID, Masouros SD, Amis AA. Biomechanics of the menisci of the knee. *Curr Orthop*
236 2008;22:193–201.
- 237 [7] Furumatsu T, Kanazawa T, Yokoyama Y, Abe N, Ozaki T. Inner meniscus cells maintain higher
238 chondrogenic phenotype compared with outer meniscus cells. *Connect Tissue Res*
239 2011;52:459–65.
- 240 [8] Halper J. Proteoglycans and Diseases of Soft Tissues. *Adv. Exp. Med. Biol.*, vol. 802, 2014, p.
241 49–58.
- 242 [9] McDevitt CA, Webber RJ. The ultrastructure and biochemistry of meniscal cartilage. *Clin*
243 *Orthop Relat Res* 1990;252:8–18.
- 244 [10] Roughley PJ, McNicol D, Santer V, Buckwalter J. The presence of a cartilage-like proteoglycan
245 in the adult human meniscus. *Biochem J* 1981;197:77–83.
- 246 [11] Mcnicol D, Roughley PJ. Extraction and Characterization of Proteoglycan from Human
247 Meniscus. *Biochem J* 1980;185:705–13.
- 248 [12] Adams ME, Muir H. The glycosaminoglycans of canine menisci. *Biochem J* 1981;197:385–9.
- 249 [13] Nakano T, Dodd CM, Scott PG. Glycosaminoglycans and proteoglycans from different zones of
250 the porcine knee meniscus. *J Orthop Res* 1997;15:213–20.
- 251 [14] Fox AJS, Wanivenhaus F, Burge AJ, Warren RF, Rodeo SA. The human meniscus: a review of
252 anatomy, function, injury, and advances in treatment. *Clin Anat* 2015;28:269–87.
- 253 [15] Canal Guterl C, Hung CT, Ateshian GA. Electrostatic and non-electrostatic contributions of
254 proteoglycans to the compressive equilibrium modulus of bovine articular cartilage. *J*
255 *Biomech* 2010;43:1343–50.
- 256 [16] Han E, Chen SS, Klich SM, Sah RL. Contribution of proteoglycan osmotic swelling pressure to
257 the compressive properties of articular cartilage. *Biophys J* 2011;101:916–24.
- 258 [17] Korhonen RK, Laasanen MS, Töyräs J, Lappalainen R, Helminen HJ, Jurvelin JS. Fibril reinforced
259 poroelastic model predicts specifically mechanical behavior of normal, proteoglycan depleted
260 and collagen degraded articular cartilage. *J Biomech* 2003;36:1373–9.
- 261 [18] Parsons JR, Black J. Mechanical behavior of articular cartilage: quantitative changes with
262 alteration of ionic environment. *J Biomech* 1979;12:765–73.
- 263 [19] Korhonen RK, Jurvelin JS. Compressive and tensile properties of articular cartilage in axial
264 loading are modulated differently by osmotic environment. *Med Eng Phys* 2010;32:155–60.
- 265 [20] Räsänen LP, Tanska P, Zbýň Š, van Donkelaar CC, Trattng S, Nieminen MT, et al. The effect of
266 fixed charge density and cartilage swelling on mechanics of knee joint cartilage during
267 simulated gait. *J Biomech* 2017;61:34–44.
- 268 [21] Wilke HJ, Neef P, Caimi M, Hoogland T, Claes LE. New in vivo measurements of pressures in
269 the intervertebral disc in daily life. *Spine (Phila Pa 1976)* 1999;24:755–62.
- 270 [22] Buckwalter JA, Smith KC, Kazarien LE, Rosenberg LC, Ungar R. Articular cartilage and
271 intervertebral disc proteoglycans differ in structure: An electron microscopic study. *J Orthop*
272 *Res* 1989;7:146–51.
- 273 [23] Heneghan P, Riches PE. The strain-dependent osmotic pressure and stiffness of the bovine
274 nucleus pulposus apportioned into ionic and non-ionic contributors. *J Biomech*
275 2008;41:2411–6.

- 276 [24] Gelber PE, Gonzalez G, Torres R, Garcia Giralto N, Caceres E, Monllau JC. Cryopreservation
277 does not alter the ultrastructure of the meniscus. *Knee Surg Sports Traumatol Arthrosc*
278 2009;17:639–44.
- 279 [25] Qu C, Hirviniemi M, Tiitu V, Jurvelin JS, Töyräs J, Lammi MJ. Effects of Freeze-Thaw Cycle with
280 and without Proteolysis Inhibitors and Cryopreservant on the Biochemical and Biomechanical
281 Properties of Articular Cartilage. *Cartilage* 2014;5:97–106.
- 282 [26] Mow VC, Schoonbeck JM. Contribution of Donnan osmotic pressure towards the biphasic
283 compressive modulus of articular cartilage. *Trans Orthop Res Soc* 1984;9:262.
- 284 [27] Maas SA, Ellis BJ, Ateshian GA, Weiss JA. FEBio: Finite Elements for Biomechanics. *J Biomech*
285 *Eng* 2012;134:011005.
- 286 [28] Holmes MH, Mow VC. The nonlinear characteristics of soft gels and hydrated connective
287 tissues in ultrafiltration. *J Biomech* 1990;23:1145–56.
- 288 [29] Ateshian GA, Warden WH, Kim JJ, Grelsamer RP, Mow VC. Finite deformation biphasic
289 material properties of bovine articular cartilage from confined compression experiments. *J*
290 *Biomech* 1997;30:1157–64.
- 291 [30] Busby GA, Grant MH, MacKay SP, Riches PE. Confined compression of collagen hydrogels. *J*
292 *Biomech* 2013;46:837–40.
- 293 [31] Iatridis JC, Setton LA, Foster RJ, Rawlins BA, Weidenbaum M, Mow VC. Degeneration affects
294 the anisotropic and nonlinear behaviors of human annulus fibrosus in compression. *J Biomech*
295 1998;31:535–44.
- 296 [32] Soltz MA, Ateshian GA. Interstitial Fluid Pressurization During Confined Compression Cyclical
297 Loading of Articular Cartilage. *J Biomech* 1998;31:927–34.
- 298 [33] Hosseini SM, Wilson W, Ito K, van Donkelaar CC. How preconditioning affects the
299 measurement of poro-viscoelastic mechanical properties in biological tissues. *Biomech Model*
300 *Mechanobiol* 2013;13:503–13.
- 301 [34] Lai WM, Hou JS, Mow VC. A triphasic theory for the swelling and deformation behaviors of
302 articular cartilage. *J Biomech Eng* 1991;113:245–58.
- 303 [35] Huyghe JM, Janssen J. Quadriphasic mechanics of swelling incompressible porous media. *Int J*
304 *Eng Sci* 1997;35:793–802.
- 305 [36] Proctor CS, Schmidt MB, Whipple RR, Kelly MA, Mow VC. Material properties of the normal
306 medial bovine meniscus. *J Orthop Res* 1989;7:771–82.
- 307
- 308

Figure Legends

Figure 1 - Mean stress relaxation curves [standard errors: 0.14M PBS +/-0.143N, deionised water +/- 0.098N, 3M PBS +/-0.1045N)

Figure 2 – Confined compression apparatus (bath allowing entire apparatus to be bathed in solution removed for clarity)

Figure 1
[Click here to download high resolution image](#)

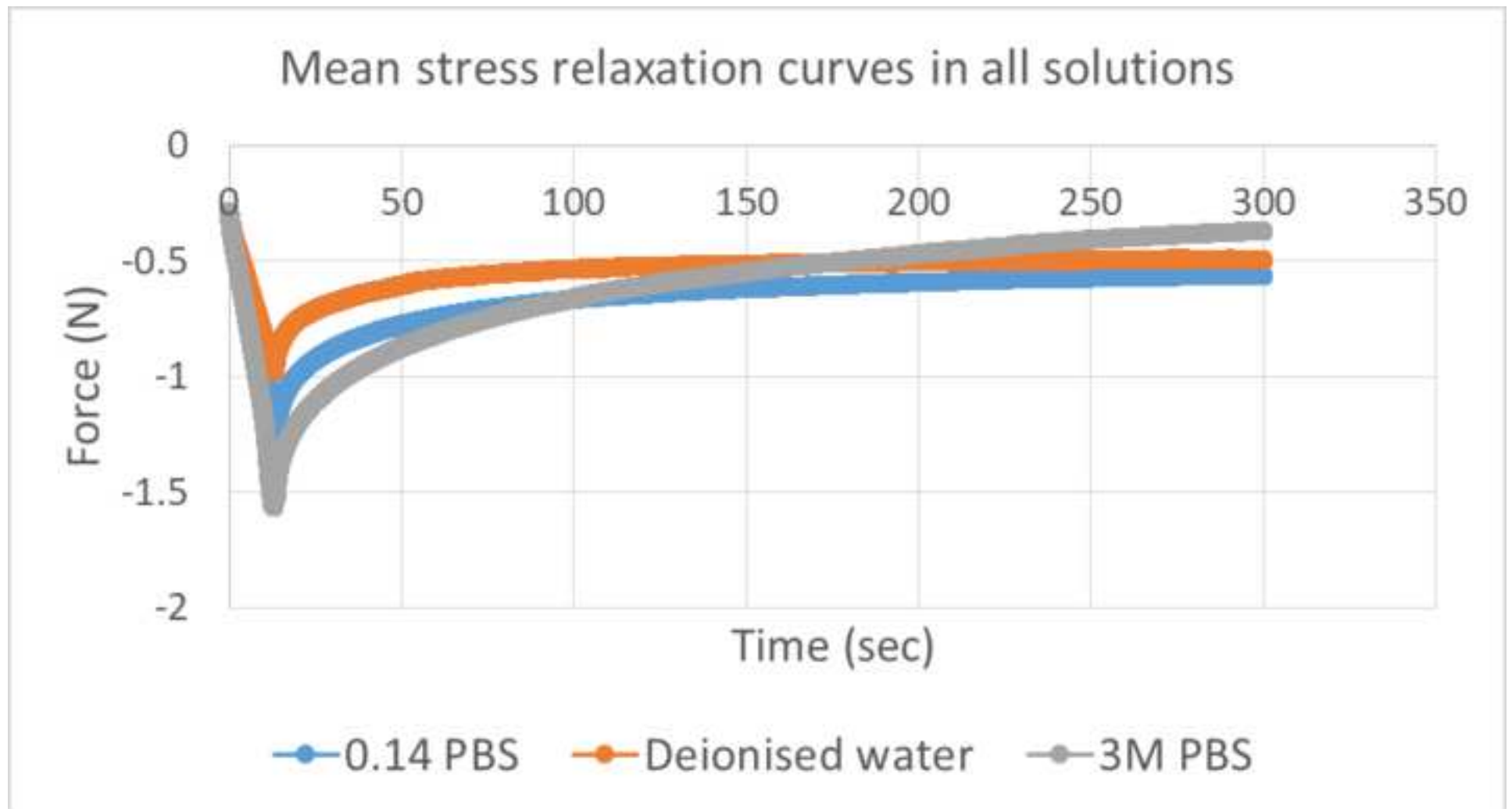


Figure 2
[Click here to download high resolution image](#)



Table 1

Mean values +/- s.d.						
Solution	E (Young's Modulus) (MPa)	K ₀ (zero strain dependent permeability) ($\times 10^{-15}$ m ⁴ /Ns)	M (exponential strain dependent coefficient)	β (exponential stiffening coefficient)	γ (viscoelastic coefficient)	τ (relaxation time)(secs)
0.14M PBS	0.42+/-0.32	0.53+/-0.39	0.00+/-0.00	0.11+/-0.19	0.55+/-0.26	68.85+/-24.39
Deionised water	0.38+/-0.23	0.89+/-0.59	0.00+/-0.00	0.00+/-0.00	0.59+/-0.18	52.30+/-19.78
3M PBS	0.09*+/-0.11	0.06*+/-0.02	0.01+/-0.03	0.27+/-0.85	0.07*+/-0.00	-

*p<0.05 compared with 0.14% PBS/deionised water

Table 1 – Comparison of derived mechanical parameters across all three solutions